

**OPTIMIZATION OF WIND-UP TENSION OF WEBS  
PREVENTING WRINKLES AND SLIPPAGE WITH  
EXPERIMENTAL VERIFICATION**

**By**

**Hiromu Hashimoto  
Tokai University  
JAPAN**

**ABSTRACT**

This paper describes the optimization method of wind-up tension to prevent wound roll defects, mainly star defect (wrinkling) and telescope (slippage), based on the optimum design technique. Hakiel's nonlinear model with air entrainment effects is applied to analyze in-roll stress distributions in the radial and tangential directions. It is well known experimentally that a decrease in the wind-up tension prevents star defects due to negative tangential stress under winding. Thus, in the present optimization method, wind-up tension is gradually decreased in the radial direction to minimize the tangential stresses under the constraint of nonnegative tangential stresses. At the same time, we consider the friction conditions to prevent the slippage between web layers due to a decrease of radial stresses and friction force. Successive quadratic programming, which is the typical mathematical programming method, is used as the optimization technique. Wind-up tension is expressed by the third-order spline curve of a radial coordinate. The linear function with respect to the radial coordinate is used as the original wind-up tension. The optimized wind-up tensions are obtained for various winding condition, and we confirmed theoretically and experimentally that the in-roll stress distributions were very much improved for preventing wrinkle and slippage by optimization method proposed.

**INTRODUCTION**

The web handling processes have been broadly used for a lot of products, such as liquid crystal display monitors (LCD), mobile phones, solar and fuel cells, and plastic/paper sheets. Most of web handling industrials are often concerned with the problems of wrinkling and the slippages in the wound roll. These web defects had been a cause of losing a lot of the materials and higher production costs, and wasting a lot of time to restore the wound roll. The generation of wrinkling and slippage in the wound roll is strongly related with the internal stresses distributions in wound roll; therefore, it is

necessary to understand well the background about stress inside the wound roll. In the past, some researchers investigated about the internal stress distribution. Gutterman[1] and Catlow et al[2] were the first group that studied with internal stress. They found out internal stress inside the roll with the theory of thick-walled cylinder and the roll was regarded as homogeneous and isotropic. Then, the boundary condition, which considered for core deformation was accurately treated by Yogoda[3]. After that Pfeiffer[4] found out the nonlinearity of the elastic Young modulus of radial direction which was verified by experimental. Therefore, Hakiel[5] was the first researcher who wrote about the nonlinear second order differential equation for the internal stress and used the finite difference method to solve the equation under the boundary equations without the air-entrainment between each thin layers. Then, Good et al[6] considered the effect of the air-entrainment in roll, and Tanimoto et al[7] and Sasaki et al[8] applied the Hakiel's model under the effect of air-entrainment to find out the in-roll stresses in paper winding system. Regarding the relationship of the wound roll defects and winding tensions, Lin and Wickert[9] showed the experimental results of the polyethyleneterephthalate substrate with coatings in which there were the wound roll defects at high winding tension.

From previous studies, it follows that higher winding tension, higher nip-load, and higher winding speed become a cause of wrinkling and slippage. High winding tension and nip load lead to the wrinkling in the wound roll because of higher radial stresses, and the higher winding speed leads to the slippage because of air entrainment between web layers; therefore, it is desired to find out the optimum winding tension and for protecting both wrinkling and slippage the wound roll system.

However, very few researches studied the optimum winding tension for preventing the wrinkling and slippage. So, it is required to find out the new technique which is able to use for solving web defect problems in the wound roll. Regarding to optimization of web winding tension, Hashimoto et al[10] had been used the successive quadratic programming method (SQP) for the optimum design of the thrust air bearing geometry, then this paper will extend this optimization technique to determine the winding tension curve for protecting the defects. The obtained results will be compared with the measured data to verify its applicability.

## NOMENCLATURE

$f(X)$	: Objective function [Pa]
$F$	: Friction force [N] between film layers of a wound roll interior
$F_{ex}$	: Axial direction external force [N] that acts on wound roll
$g_i(X) (i = 1 \sim 2n+1)$	: Constraint function
$h$	: Thickness [m] of air layer at time of winding
$h_0$	: Thickness [m] of the air layer of the outermost layer of the roll
$g$	: Parameter defined by Eq. (3)
$C_0 \sim C_2$	: Coefficient in Eq. (7)
$L$	: Nip load (=N/W) [N/m] per unit width
$N$	: Nip load [N]
$Pa$	: Air pressure [Pa]
$r$	: Roll radius [m] at time of winding
$r_c$	: radius of a winding core [m]
$r_{max}$	: Maximum diameter [m] of roll
$R_{eq}$	: Equivalent radius [m] of a wound roll and a nip roll
$R_{nip}$	: Radius [m] of a nip roll
$s$	: Outermost circumference radius [m] of a wound roll
$t_f$	: Thickness [m] of partially wound up film

$t_{f0}$	: Thickness [m] of film at the time of commencement of winding
$T_w(r)$	: Wind-up tension function [N/m]
$T_{we}$	: Wind-up tension [N/m] at $r = rc$
$T_{ws}$	: Wind-up tension [N/m] at $r = r_{max}$
$T_{w0}(r)$	: Initial wind-up tension function [N/m]
$\delta i(i = 1 \sim n)$	: Tension variation [N/m] in the making at the $i$ th node
$\Delta T_i(i = 1 \sim n)$	: Variation [N/m] from initially set tension at the $i$ th node
$U_w$	: Winding-up velocity [m/s] of film
$W$	: Film width [m]
$X$	: Design variable vector
$\epsilon_r$	: Radial direction strain of take-up roll
$\eta$	: Viscosity [Pa·s] of air
$\mu_{ff}$	: Boundary friction coefficient between film layers
$\nu_{nip}$	: Poisson's ratio of nip roll
$\nu_{rt}$	: Poisson's ratio of take-up roll
$\sigma_{ff}$	: Composite surface roughness [m] between film layers
$\sigma_r$	: Radial direction stress [Pa] of wound roll interior
$\delta\sigma_r$	: Increment [Pa] of radial direction stress
$\sigma_t$	: Circumferential direction stress [Pa] of wound roll interior
$\varphi$	: Taper ratio of wind-up tension

### ANALYTICAL MODEL OF THE INTERNAL STRESS OF A ROLL

Figure 3(a) is a conceptual diagram of the most basic center drive winding that does not use a nip roll among the winding systems presently used. Because it has been confirmed that the Hakiel model [9] is effective with respect to this kind of winding system, in this research this model is used where air entrainment is involved. A summary of the model is described below.

Modeling prerequisites are as follows: (1) a wound roll is a perfect cylinder, and the film thickness is uniform; (2) as for the internal stress of a wound roll, the radial and circumferential direction stresses are controlling, and the influence of the roll axial direction stress can be ignored; (3) we can ignore the shear stress between film layers; (4) the effect of film wound in a spiral shape can be ignored, the wound roll can be represented by an accumulation of thin-walled cylinders, and similar assumptions are provided. The radial direction stress  $\sigma_{ri}$  at the  $i$ th layer of a roll wound under these kinds of assumptions is found adding all stress increments in each layer from the  $i+1$  layer up to the  $n$ th layer (final layer of winding) and is represented by Eq. {1}. In which  $i$ -th layer means that the layer at the winding core is regarded as the first and represents the  $i$ th layer when counted in sequence the outer layer.

$$\sigma_{r,i} = \sum_{j=i+1}^n \delta\sigma_{r,j} \quad \{1\}$$

Here,  $\delta\sigma_{rij}$  represents the stress increment in the  $j$ th layer when wound up to the  $i$ th layer, and the equation that controls  $\delta\sigma_{ri}$  is given as follows.

$$r^2 \frac{d^2 \delta \sigma_r}{dr^2} + (3 - \nu_{rt}) r \frac{d \delta \sigma_r}{dr} + (1 + \nu_{rt} - g^2) \delta \sigma_r = 0 \quad \{2\}$$

Provided that parameter  $g$  is defined by the following equation

$$g = \sqrt{\frac{E_t}{E_r}} \quad \{3\}$$

The boundary conditions in the outermost circumference and the innermost circumference of the roll, respectively, are set as follows.

$$\delta \sigma_r \Big|_{r=s} = -\frac{T_w \Big|_{r=s}}{s} \quad \{4\}$$

$$\frac{d \delta \sigma_r}{dr} \Big|_{r=r_c} = \left( \frac{E_t}{E_c} - 1 + \nu_{rt} \right) \frac{\delta \sigma_r \Big|_{r=r_c}}{r_c} \quad \{5\}$$

The circumferential direction stress  $\sigma_t$  can be found from the following equation using the radial direction stress  $\sigma_r$  that can be obtained from Eqs. {1}-{5}

$$\sigma_t = r \frac{d \sigma_r}{dr} + \sigma_r \quad \{6\}$$

Now, the fact that the relationship of the radial direction stress  $\sigma_r$  of a wound roll interior and Young's modulus  $E_r$  becomes nonlinear, and that relationship is represented by the following equation.

$$E_r = C_0 + C_1 |\sigma_r|^{C_2} \quad \{7\}$$

Provided that the coefficients  $C_0$ - $C_2$  in Eq. {7} are constants that can be found experimentally. In the film-carrying step, there are also many cases of carrying out surface treatment by physical vapor deposition and chemical vapor deposition. In this case, it is acceptable to think that there is no entrainment of air in the wound roll interior the atmosphere is in an environment close to a vacuum. Consequently, the stress distribution of the roll interior can be determined by solving Eqs. {1}-{6}. However, in the case of normal winding in air, the entrainment of air cannot be avoided, an air layer is formed between the film layers, and, because Young's modulus of the radial direction of the roll is lowered due to its influence, it is necessary to take this effect into consideration.

In the case of center drive winding shown in Fig.3(a), it is possible to represent the relationship of the film that can be wound and the already-wound roll part using a foil-bearing model. This problem has already been formulated by Hashimoto [11], and the initial air-film thickness  $h_0$  at the time of winding can be found by the following equation.

$$h_0 = 0.589s \left( \frac{12\eta U_w}{T_w} \right)^{2/3} \quad \{8\}$$

Provided that the amount of the outflow of air from the end of the roll is ignored because it is minute.

Here, according to Good[6] and Tanimoto[7], by using the relationship of the stress and strain of the equivalent layer of the collective thickness( $t_f + h_0$ ) of the initial film thickness  $t_f$  and the air film thickness  $h_0$  and Boyle's law, the radial direction equivalent of Young's modulus  $E_{req}$  that has taken into consideration air entrainment can be found as follows.

$$E_{req} = \frac{t_f + h_0}{\frac{t_f}{E_r} + \frac{h_0}{E_{ra}}} \quad \{9\}$$

Provided that Young's modulus  $E_{ra}$  of the air layer can be given as follows.

$$E_{ra} = \frac{(|\sigma_r| + P_a)^2}{T_w|_{r=s} / s + P_a} \quad \{10\}$$

Meanwhile, the equivalent Young's modulus  $E_{teq}$  of the circumferential direction of a wound roll can be found using the following equation.

$$E_{teq} = \frac{t_f}{t_f + h} E_t \quad \{11\}$$

Here, in the process of winding, film thickness  $t_f$  and thickness  $h$  of the air film can be given as follows.

$$t_f = t_{f0} \left( 1 - \frac{\delta\sigma_r}{E_r} \right) \quad \{12\}$$

$$h = \left( \frac{T_w|_{r=s} / s + P_a}{|\sigma_r| + P_a} \right) h_0 \quad \{13\}$$

According to the above, in the center drive winding shown in Fig. 3(a) the internal stress of a wound roll when air entrainment is taken into consideration can be determined using the equivalent Young's moduli  $E_{req}$  and  $E_{teq}$  that can be given by Eqs. {9} and {11}, respectively, instead of Young's moduli  $E_r$  and  $E_t$  of Eqs. {1}-{6}.

Now, generally, when air is entrained at the time of film winding, as is also clear by the analytical result shown later, the pressure between the film layers of the wound roll interior lowers, and a slip occurs easily. Accordingly, for the purpose of causing the amount of entrained air to be decreased as much as possible and preventing slip, center drive winding is often carried out using a nip roll shown in Fig. 3(b). The initial entrained air film thickness  $h_0$  of this case can be evaluated by the elasto-hydrodynamic theory of

the line contact between the wound roll and the nip roll. In this research, the result of Hamrock and Dowson [13] shown next is used.

$$h_0 = 7.34R_{eq} \left( \frac{\eta U_w}{E_{eq} R_{eq}} \right)^{0.65} \left( \frac{N}{E_{eq} R_{eq}^2} \right)^{-0.23} \quad \{14\}$$

Here, the equivalent radius  $R_{eq}$  and equivalent Young's modulus  $E_{eq}$  of the wound roll and the nip roll can be given by Eqs. {15} and {16}.

$$R_{eq} = \frac{1}{\frac{1}{s} + \frac{1}{R_{nip}}} \quad \{15\}$$

$$E_{eq} = \frac{1}{\frac{1 - \nu_{r\theta}^2}{E_r|_{r=s}} + \frac{1 - \nu_{nip}^2}{E_{nip}}} \quad \{16\}$$

Using the initial air film thickness  $h_0$  that can be found by Eq. {14}, the equivalent Young's moduli  $E_{req}$  and  $E_{teq}$  of the radial and circumferential directions respectively, that have taken into consideration the influence of the entrained air mentioned above can be obtained from Eqs. {9} – {13}. Consequently, the internal stress distribution of the wound roll can be determined by applying these values in Eqs. {1}–{6}.

According to Good et al. [6], the wind-up tension  $T_w$  when a nondriving nip wheel is used can be given by Eq. {17}, which takes into consideration the induced tension attributable to friction at the nip part. Furthermore, there is the necessity of taking the case of driving a nip wheel into consideration and the tension changes at the nip part, but because a nondriving nip wheel is discussed in this article, this influence is not considered.

$$T_w = T_{w0} + \mu_k L \quad \{17\}$$

Here,  $T_{w0}$  is the initial wind-up tension, and  $\mu_k$  is the dynamic friction coefficient that takes the influence of air entrainment into consideration that can be found using Eq. {18}.

$$\mu_k = \begin{cases} \mu_s & (h > \sigma_{ff}) \\ \frac{\mu_s}{2} \left( 3 - \frac{h}{\sigma_{ff}} \right) & (\sigma_{ff} \leq h \leq 3\sigma_{ff}) \\ 0 & (h > 3\sigma_{ff}) \end{cases} \quad \{18\}$$

Here,  $\mu_k$  is the boundary friction coefficient between film layers, and  $\sigma_{ff}$  is the composite surface roughness of film layers defined by the following equation.

$$\sigma_{ff} = \sqrt{\sigma_{f1}^2 + \sigma_{f2}^2} \quad \{19\}$$

However, subscripts 1 and 2 indicate the roughness of the film front surface and back surface, respectively.

## OPTIMIZATION METHOD OF WINDING TENSION CURVE

The size of the wind-up tension is a parameter that exerts a large influence at the time of optimizing the stress in roll, which is the main cause of a roll defect. Accordingly, in this article we apply an investigation from the viewpoint of the optimization of the wind-up tension, concerning an effective method of preventing the star defect (wrinkle) and telescope (slippage) that have a comparatively high frequency of occurrence, even among roll defects. That method is described below.

For a long time, method of causing wind-up tension  $T_w$  to decrease in proportion to the roll radial  $r$  have been used to prevent the occurrence of a star defect. As tension-decrease methods, the method that follows a straight line (at the production site often called the taper tension) and the method that follows a hyperbolic curve are common. However, these tension functions are established depending on experience, and there is not always a theoretical guarantee that they are optimal wind-up tensions. Accordingly, in this article, on condition that the minimum value of the tangential direction stress of the wound roll interior  $\sigma_t$  becomes nonnegative, the tension function  $T_w(r)$  so that the average value of the radial direction of  $\sigma_r$  becomes the minimum is determined applying the method of optimization of the groove shape of a thrust air bearing that Hashimoto et al.[10] already proposed.

At the time of winding tension optimization, the method that sets the taper tension that causes the tension to linearly decrease as the initial tension function and causes the tension function to gradually evolve so that the circumferential direction stress  $\sigma_t$  becomes the minimum and nonnegative is used as the objective function. In dealing with the expression of a common tension function  $T_w(r)$ , taking into consideration the flexibility and ease of handling of a function, the cubic spline function shown next is used.

Here Eq{20} the symbol  $\Delta r$  is an equally divided section of the radial direction coordinate  $r$ , and  $M_i$  is the shape parameter determined from the condition in which the first derivative becomes continuous at each node position of the curve that is represented in each section.

$$T_w(r) = \frac{M_i}{6\Delta r}(r_{i+1} - r)^3 + \frac{M_i}{6\Delta r}(r - r_i)^3 + \left(T_i - \frac{M_i\Delta r^2}{6}\right)\left(\frac{r_{i+1} - r}{\Delta r}\right) - \left(T_{i+1} - \frac{M_{i+1}\Delta r^2}{6}\right)\left(\frac{r - r_i}{\Delta r}\right) \quad \{20\}$$

When the tension function  $T_w(r)$  is caused to evolve sequentially, the  $r$  coordinate of each contact point  $P^{(k)}(r_i, T_i)$  is fixed with respect to the tension function of the previous stage ( $k$  step) in the evolutive process ( $(k+1)$  step), shown by the broken lines in Fig. 4, and the  $T_w$  coordinate is caused to change only  $\delta T_i$  in the positive direction or the negative direction and obtain a new contact point  $P_{i,(k+1)}(r_i + T_i + \delta T_i)$ . The function form is updated by Eq. {20} using the new coordinate value that could be obtained in this way and is caused to sequentially evolve until the value of the objective function  $f(X)$  mentioned later becomes optimum.

Because of the above, at the time of optimization of the wind-up tension, the design variable vectors are set as follows.

$$X = (\Delta T_1, \Delta T_2, \Delta T_3, \dots, \Delta T_n) \quad \{21\}$$

However, divide  $(n + 1)$  in the  $r$  direction from the winding core position up to the outermost diameter. Furthermore,  $\Delta T_i$  indicates the difference of the initially set tension  $T_{w0}$  at an arbitrary radius position  $r_i$  with the partially evolved ( $k$  step) tension.

The objective function  $f(X)$  is defined by the following equation.

$$f(X) = \sum_{i=1}^{\max} \left\{ \left( \frac{F_i}{F_{ref}} - 1 \right)^2 + \left( \frac{\sigma_{t,i}}{\sigma_{t,ref}} \right)^2 \right\} \quad \{22\}$$

Where  $F_i$  the friction force between web layers,  $F_{ref}$  is the critical friction force to start the slippage, which is determined experimentally in this paper as  $F_{ref} = 5 \times 103N$  (equivalent to the impact acceleration of 50g), and  $\sigma_{t,ref}$  shows the reference value of tangential stress.  $F_i$  and  $F_{ref}$  are, respectively, calculated by Eqs. {23} and {24}.

$$F_i = 2\pi r_i \mu_k |\sigma_{r,i}| W \quad \{23\}$$

$$\sigma_{t,ref} = \frac{T_{w0}}{t_{w0}} \quad \{24\}$$

On the other hand, a limiting condition that can be imposed on the circumferential direction stress  $\sigma_t$  that is a design variable  $\Delta T_i (i = 1 \sim n)$  and quantity of state regards the upper and lower limit values of the design variable  $\Delta T_i$ , the friction condition, and the minimum value  $\sigma_{t,min}$  of the circumferential direction stress  $\sigma_t$  as nonnegative and represents these by the following inequality expression.

$$g_i(X) \geq 0 \quad (i = 1 \sim 2n + 2) \quad \{25\}$$

However, the constraint function  $g_i(X) (i = 1 \sim 2n + 1)$  is regarded as being able to be given as follows.

$$\left. \begin{array}{l} g_1 = \Delta T_1, g_2 = T_{w0} - \Delta T_1 \\ g_3 = \Delta T_2, g_4 = T_{w0} - \Delta T_2 \\ \cdot \\ \cdot \\ g_{2n-1} = \Delta T_n, g_{2n} = T_{w0} - \Delta T_n \\ g_{2n+1} = \sigma_{t,min}, g_{2n+2} = F_i - F_{ref} \end{array} \right\} \geq 0 \quad \{26\}$$

Furthermore, in this article, set at  $\Delta T_{imin} = 0, (i=1 \sim n)$ , optimization is attempted. From this the problem of wind-up tension is defined as follows.



$$\begin{aligned} &\text{Find } X \text{ to minimize } f(X) \\ &\text{Subject to } g_i(X) \geq 0 \quad (i = 1 \sim 2n + 2) \end{aligned} \quad \{27\}$$

## EXPERIMENT

The experiments consist of measuring the radial stresses in the wound roll and the impact load test after winding to observe whether the slippage will occur or not. Figure 5 shows the diagram of a winding machine which has the control system to control the winding tensions including both linear and non-linear tensions, nip-loads, and web velocities. The thin film (PET) is transferred from the wound out roll and passing through the pinch roller, and nip roller, and reeled finally. During the operation of winding, the force-sensitive resistors with cover film are inserted into the winding roll for measuring the radial stresses. When the force is applied on the sensor, the resistance would be changed, and then, by measuring the resistance, the radial stresses can be indirectly known with the calibration result of the relation between pressure and resistance. The force-sensitive resistor used here is shown in Fig. 6.

As can be seen in Fig. 6, the sensor is covered with film. In the previous research works, the force-sensitive resistor without cover film has been used mainly for measuring the in-roll radial stresses. In this case, the stress concentration occurs at the sensing part and it leads to higher radial stress than another part as shown in Fig. 7(a). To avoid this serious problem, we propose to use the modified sensor with cover film as shown in Fig. 6. Using this type of modified sensor, the stress concentration can be avoided as shown in Fig. 7(b).

The comparison of radial stresses in the wound roll in the cases of using the sensor without and with cover films are presented in Figure 8 accompanied with the predicted results based on the analytical model presented in the former chapter. Fig. 8 shows that the radial stresses obtained by the sensor with cover film agree with the predicted results much better than the stresses measured by the sensor without cover film.

The impact load test procedure to confirm the occurrence of slippage in wound roll is illustrated in the Fig. 9. The left hand side of the figure shows the testing of slippage by falling the wound roll down to the base, in which the distance  $l_r$  is set at 10 cm (equivalent to the impact of 50g). After the wound roll was crashed against the base, the slippage along the radial direction is observed and measured by the optical sensor (LDV) as shown in Fig. 9.

## MEASURED AND PREDICTED RESULTS

In this work, the PET film was used as a test web. The physical properties of PET film, core roller, and nip-roller are shown in Table 1. The measured and predicted results concerning with the in-roll stress distributions, air-film thickness in roll, the friction force under the constant, taper, and optimum winding tensions will be presented in the following. The experimental results of the tangential stresses and friction forces in the wound roll are obtained from Eqs. {6} and {23}, indirectly by using the appropriate fitting curve of the experimental data of radial stresses.

Figure 10 shows the influence of nip-load on some physical quantities under the constant winding tension of 150 N/m, and a web velocity of 0.5 m/s. Figure 10(a) shows that the radial stress for higher nip-load of 100 N becomes higher than that for lower nip-load of 25 N. Moreover, the air film thickness becomes smaller at the higher nip-load of 100 N as shown in Fig 10(c). As the results, the friction force in the wound roll is

increased due to an increase of radial stress and a decrease of air-film thickness in the roll as shown in Fig. 10(d). From Fig. 10(d), in both cases of nip-loads of 100 N and 25 N, the friction force becomes higher than the critical slippage line ( $F_{cr}=5 \times 10^3 \text{N}$ ); thus, the slippage is hard to appear in wound roll. However, Fig. 10(b) shows the generation of negative tangential stresses in the case of higher nip-load of 100 N; and it will be possible to generate the wrinkling in the wound roll.

At the next step, the effect of taper winding tension was studied in order to change the negative tangential stresses to the positive stresses. Figure 11 shows the in-roll stress distributions, air film thickness, and friction force in the wound roll under the taper winding tensions with different taper ratio of 0, 0.4, and 0.8. As shown in Fig. 11(a), in the cases of taper ratio of 0.4 and 0.8, the radial stresses become lower than the case of constant winding tension, and then the tangential stresses become positive that could prevent the wrinkling in the wound roll as shown in Fig. 11(b). However, Figs. 11(c) and 11(d) respectively show an increase of air-entrainment and a decrease of the friction forces in the wound roll when the taper ratio is set at 0.4 and 0.8. Especially in the case of taper ratio of 0.8, the friction force at the normalized radial range from 1.8 to 2.0 becomes smaller than the critical slippage line, and in such region the slippage is easy to occur.

From the above results obtained for both cases of constant and taper winding tension, it follows that the taper tension has an advantage of preventing the wrinkle but has disadvantage of occurrence of slippage. Therefore, the development of optimum winding-up tension technique instead of taper tension winding as introduced in the former chapter is required to protect both wrinkling and slippage. Some examples showing the effectiveness of optimized tension are presented in Figs. 12 and 13. Figures 12(b) to 12(d) shows the comparison of predicted and measured results for the constant and optimized winding tensions shown in Fig. 12(a), the radial stresses under the optimized winding tension become lower than the stresses under the constant tension, and the tangential stresses are not below zero as shown in Fig. 12(c). This type of tangential stress distribution has an advantage to prevent the wrinkling in the wound roll. In addition, Fig. 12(d) shows the possibility of preventing the slippage in the wound roll due to the suitable level of friction force more than the critical line. Furthermore, Figure 14 shows clearly the amount of slippage in the wound roll after the impact load testing is very small under the optimized tension.

In the cases of different winding velocities of  $U_w=0.5 \text{ m/s}$  and  $1.0 \text{ m/s}$ , the optimized winding tension at the web velocity of  $U_w=1.0 \text{ m/s}$  becomes little higher than the tension at  $U_w=0.5 \text{ m/s}$  as shown in Fig. 14(a) because the effect of air-entrainment increases when the web velocity becomes lower. In order to prevent slippage and to increase the friction force in the wound roll at the higher winding velocity, the optimized winding tension must still be higher than the tension at  $U_w=0.5 \text{ m/s}$ . Consequently, as shown in Fig. 14(b), the radial stresses at the web velocity of  $1.0 \text{ m/s}$  are slightly lower than those at the web velocity of  $0.5 \text{ m/s}$  and the tangential stresses for all winding region become positive as shown in Fig 14(c), that could prevent for wrinkling. Figure 14(d) shows that the predicted results of friction forces for the web velocities of  $1.0 \text{ m/s}$  and  $0.5 \text{ m/s}$  at the normalized radial region from 1.0 to 1.95 become higher than the critical slippage line.

## CONCLUSIONS

This article discussed method of preventing the defects of wound rolls, a serious technical problem that should be solved as quickly as possible when producing functional films, such as optical film, by optimizing winding tension. The main conclusions obtained are set forth below.

- (1) We presented a method of representing an arbitrary winding tension function by a cubic spline function concerning radial direction coordinates and caused this to change gradually using an optimization method to realize a circumferential direction stress distribution in which a star defect and creep do not occur.
- (2) We show that the method presented in (1) is particularly effective in center drive winding in a vacuum where there is no air entrainment and in center drive winding in air that used a nip roll.
- (3) Based on the results of (1) and (2), we presented a winding tension optimization method that, together with improving the circumferential direction stress and the friction characteristics between film layers that are in a trade-off relationship with this, prevents a star defect, telescope, gauge band, and similar diverse roll defects.
- (4) The predicted results based on the above method agreed well with the measured results, and the effectiveness of winding tension optimization method proposed in this paper was verified experimentally.

## REFERENCES

1. Gutterman, R.P., "Theoretical and Practical Studies of Magnetic Tape Winding Tensions and Environmental Roll Stability," US Contract No. DA-18-119-sc-42, 1959.
2. Catlow, M.G. and Walls, G.W., "A Stability of Stress Distribution in Pirns," Journal of Textile Institute, Part 3, 1962, pp. 410-429.
3. Yogoda, H.P., "Integral Formulas for Wound Rolls," Mechanic Research Communications, Vol.7, No.2, 1980, pp.103-112.
4. Pfeiffer, J.D., "Internal Pressures in a Wound Roll," Tappi Journal, Vol.49, No.8, 1966, pp. 342-343.
5. Hakiel, Z., "Nonlinear Model for Wound Roll Stresses," Tappi Journal, Vol.70, No.5, 1997, pp. 113-117.
6. Good, J.K. and Covell, S.M., "Air Entrainment and Residual Stresses in Rolls Wound with a Rider Roll," Proceedings of the 3<sup>rd</sup> International Conference on Web Handling, 1995, pp.95-112.
7. Tanimoto, K., Kohno, K., Takahashi, S., Sasaki, M., and Yoshida, F., "Wound Stress of Permeable Papers with Air-Entrainment," Archive of Applied Mechanics, Vol.73, 2003, pp. 160-170.
8. Sasaki, M., Tanimoto, K., Kohno, K., Takahashi, S., Kometani, H., and Hashimoto, H., "In-Roll Stress Analysis considering Air-Entrainment at the Roll-Inlet with the Effect of Grooves on Nip Roll Surface," JSME J. Advanced Mechanical Design, Vol.2, 2008, pp.133-145.
9. Lin, P.M. and Wickert, J.A., "Corrugation and Buckling Defects in Wound Rolls," Journal of Manufacturing Science and Engineering ASME, Vol.128, 2006, pp.56-64.
10. Hashimoto, H. and Ochiai, M., "Optimization of Groove Geometry for Thrust Air Bearing to Maximize Bearing Stiffness," Journal of Tribology ASME, Vol.130, 2008, pp. 1-11.
11. Hashimoto H., "Air Film Thickness Estimation in Web Handling Process," Journal of Tribology ASME, Vol.121, 1999, pp. 50-55.
12. Good, J.K. and Wu, Z., "The Mechanism of Nip-Induced Tension in Wound Rolls," Journal of Applied Mechanics ASME, Vol.60, 1993, pp. 942-947.

13. Hamrock, B.J. and Dowson, D., "Elastohydrodynamic Lubrication of Elliptical contacts to Materials of Low Modulus I-Fully Flooded Conjunction," ASME J. Lubrication Technology, Vol.100, 1978, pp. 236-245.

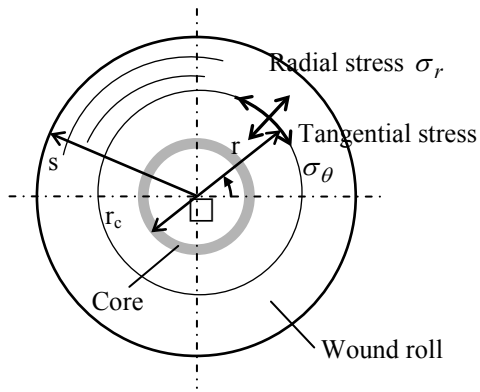
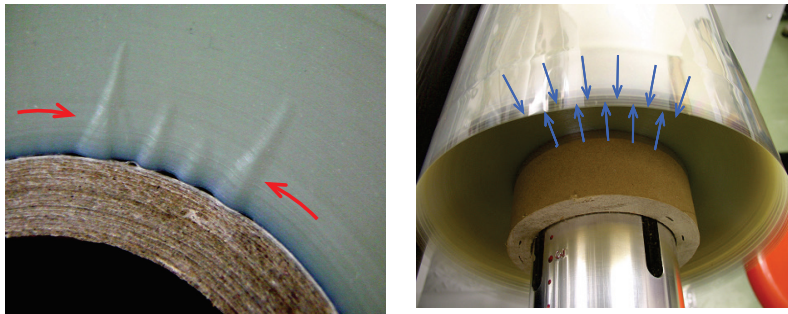


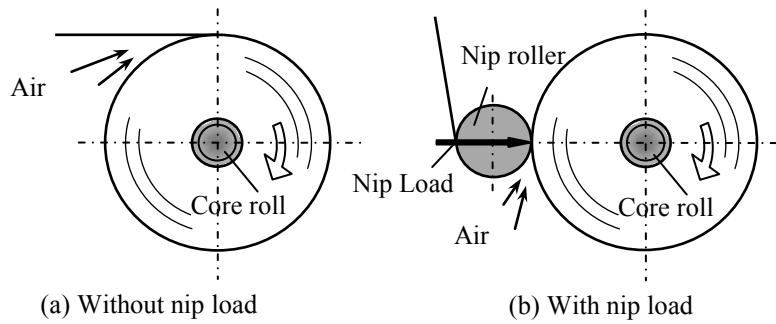
Figure 1 – In-roll stresses



(a) Wrinkling

(b) Slippage

Figure 2 – Typical of defects in wound roll



(a) Without nip load

(b) With nip load

Figure 3 – Web winding system

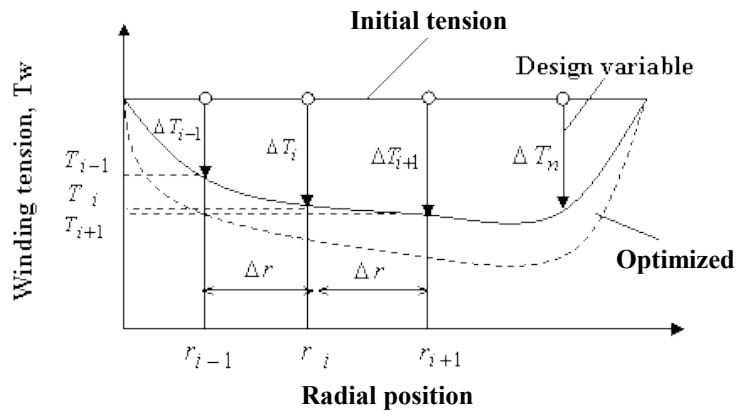


Figure 4 – Optimizing process of winding tension

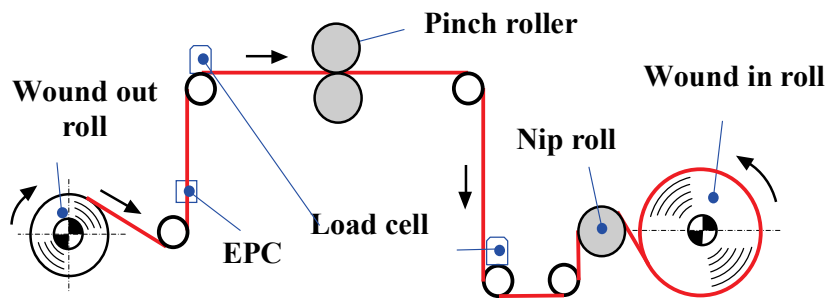
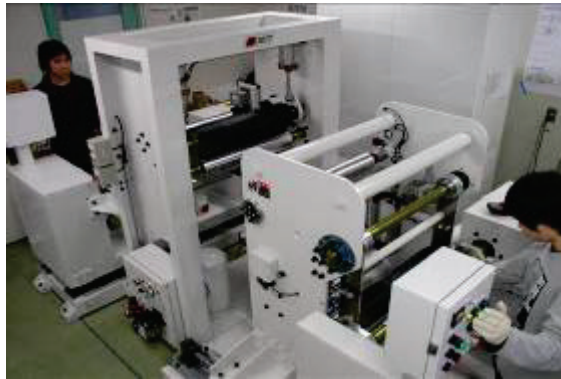


Figure 5 – Experimental apparatus

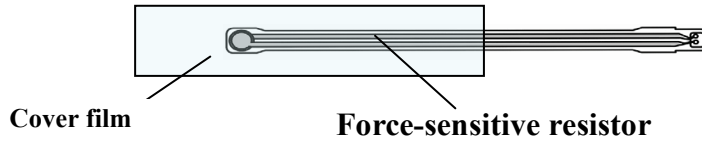


Figure 6 – The force-sensitive resistor modified with cover film

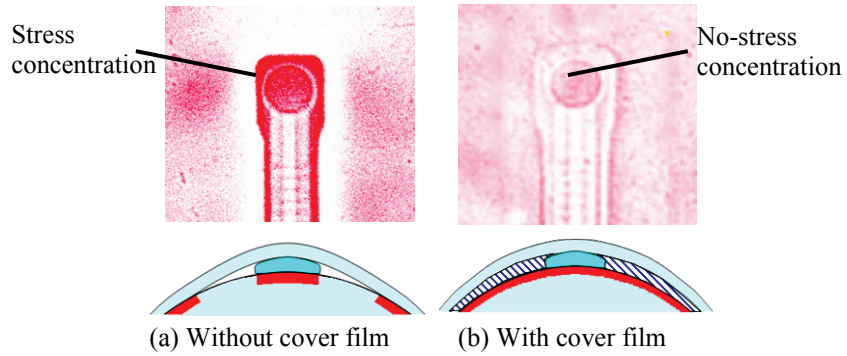


Figure 7 – Check of stress concentration at sensing part

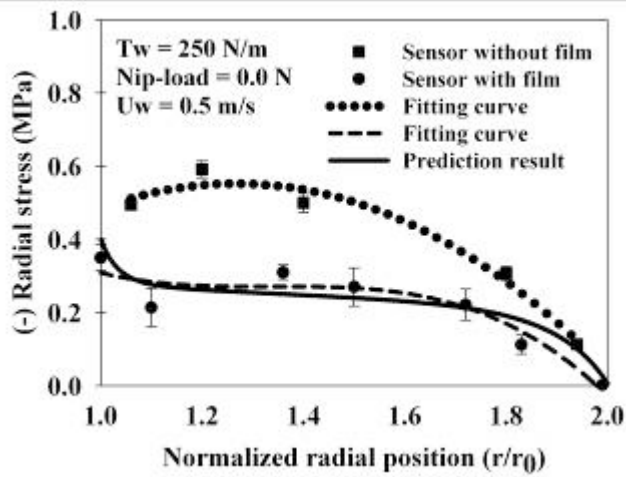


Figure 8– The comparison of radial stresses

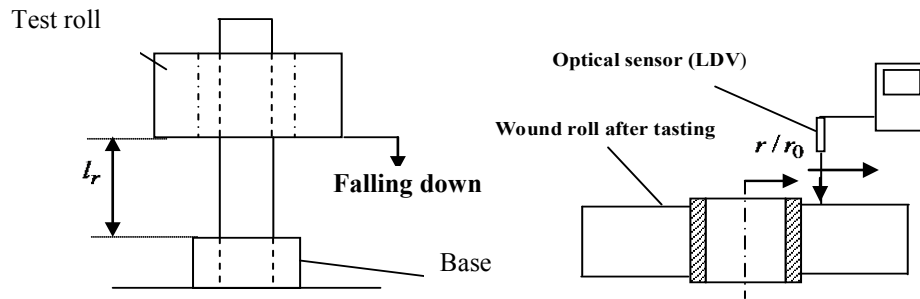
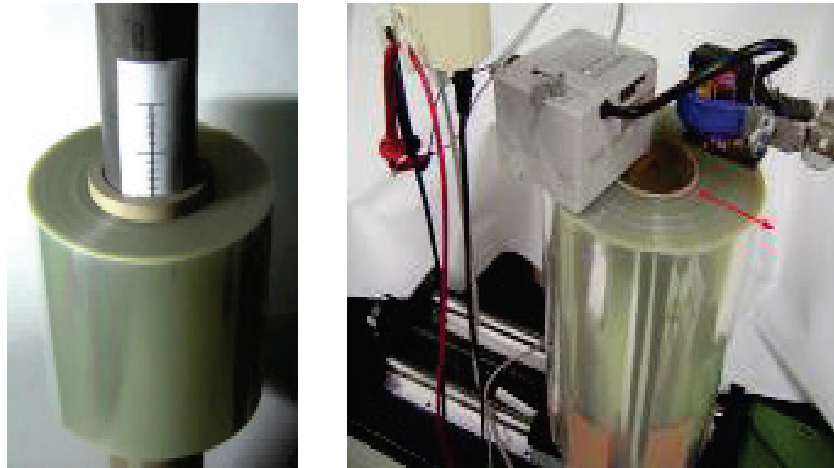
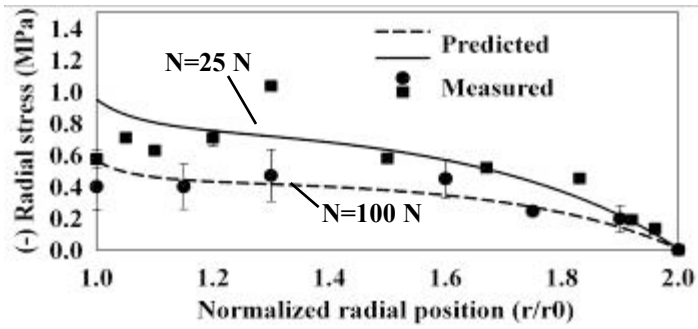


Figure 9 –Impact load test for generating slippage

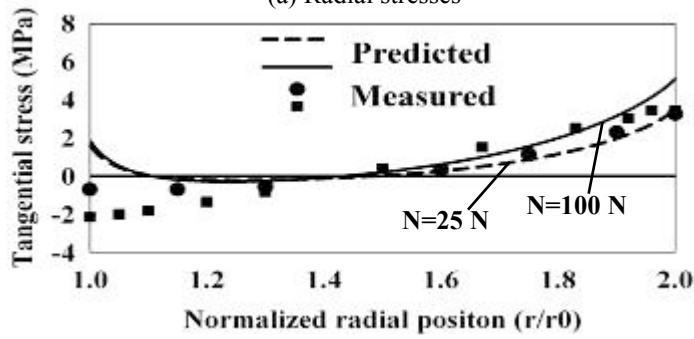
Table 1. – Physical properties of test materials

Composite RMS roughness ( $\mu m$ )	0.066		
Web thickness ( $\mu m$ )	50		
Web width (m)	0.28		
Friction coefficient	0.3		
$E_0$ (GPa)	4.80		
$\nu_{r0}$	0.3		
Core stiffness (GPa)	1.3		
Core radius (m)	0.05		
Young's modulus of nip-roll (GPa)	206		
$E_r = C_0 + C_1 \sigma_r^{C_2}$			
$E_r$	$C_0$	$C_1$	$C_2$
PET-film	0	4.09E04	0.65

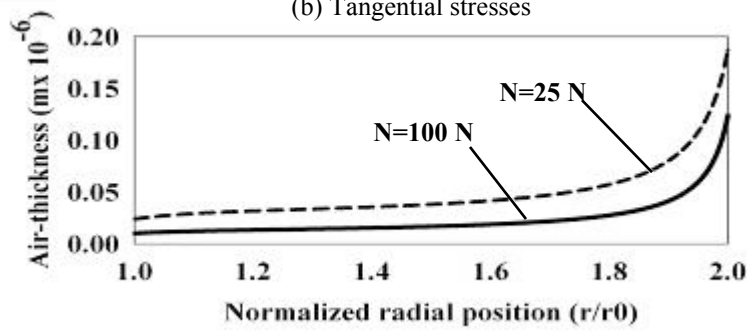




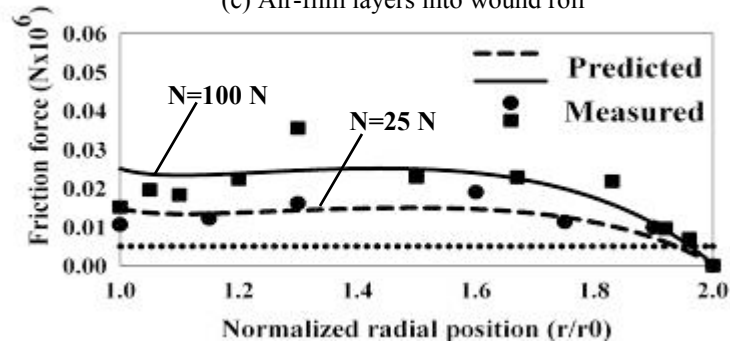
(a) Radial stresses



(b) Tangential stresses



(c) Air-film layers into wound roll



(d) Friction force

Figure 10 – Effects of nip-load on physical quantities in wound roll for  $T_w=150$  N/m,  $U_w=0.5$  m/s

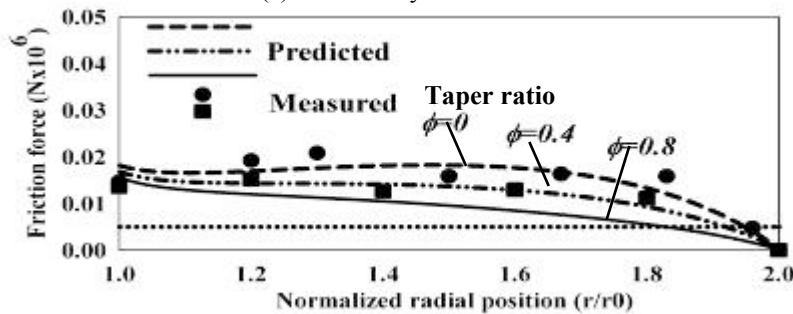
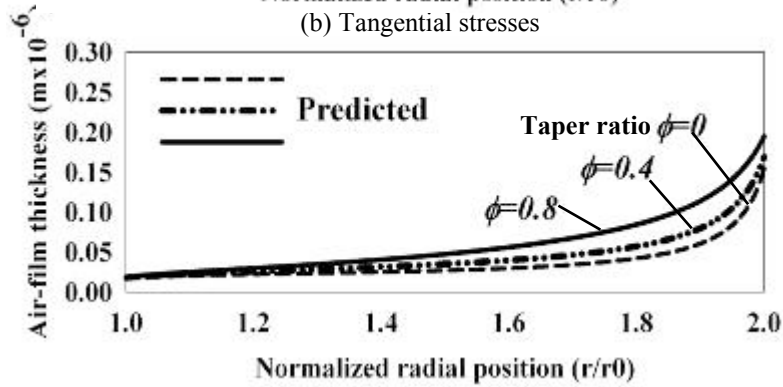
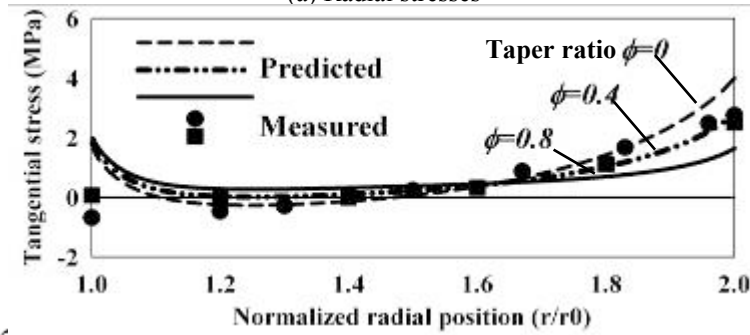
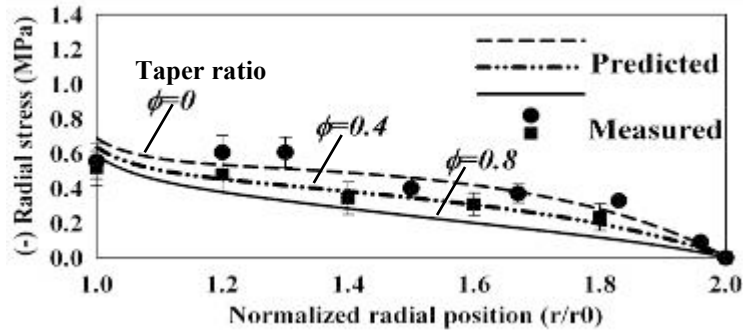
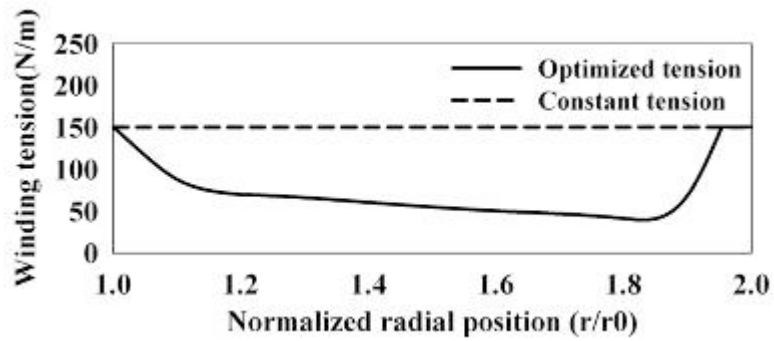
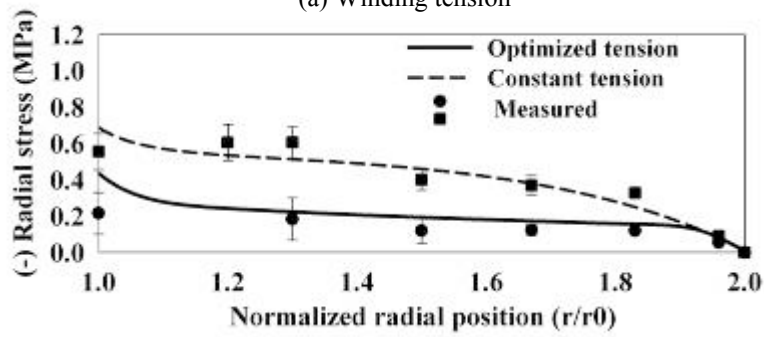


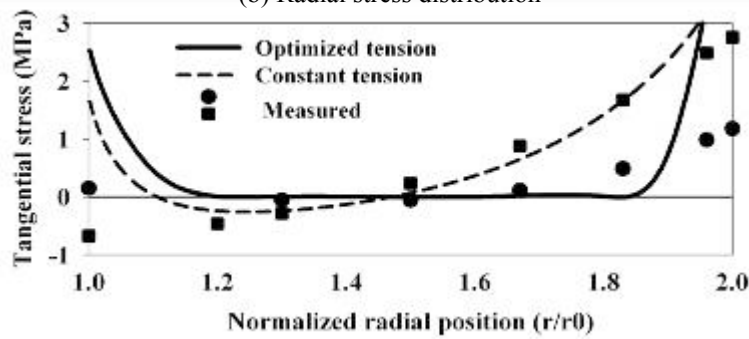
Figure 11 – Effects of taper tension on physical quantities in wound roll for  $T_w=150 \text{ N/m}$ ,  $U_w=0.5\text{m/s}$



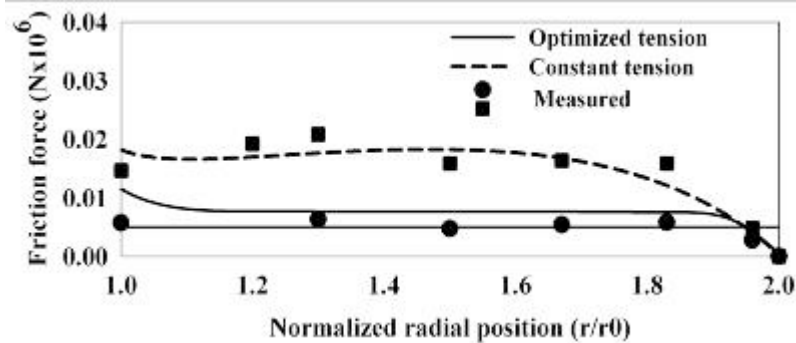
(a) Winding tension



(b) Radial stress distribution



(c) Tangential stress distribution



(d) Friction force distribution

Figure 12 – Effects of optimized tension on physical properties in wound roll for  $N=50$  N,  $U_w=0.5$  m/s



Taper tension



Optimized tension

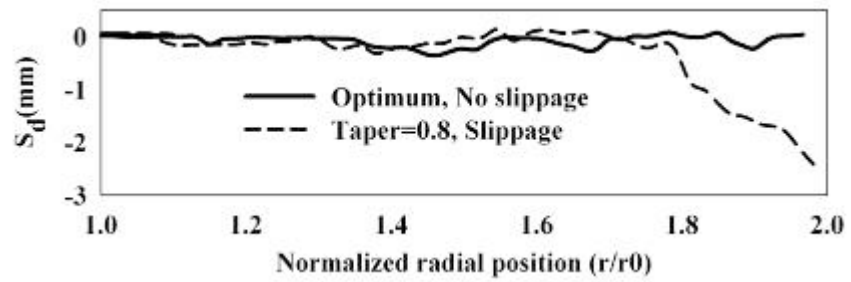
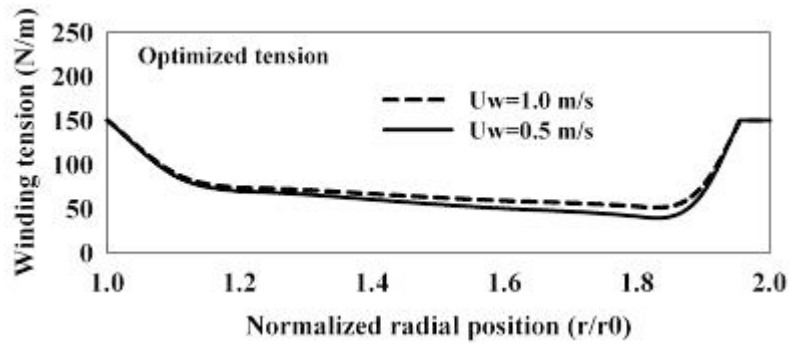
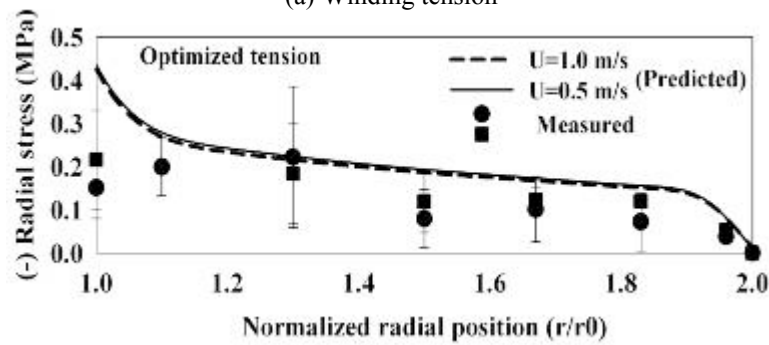


Figure 13 – Slippage after impact load test for  $N=50$  N,  $U_w=0.5$  m/s



(a) Winding tension



(b) Radial stress distribution

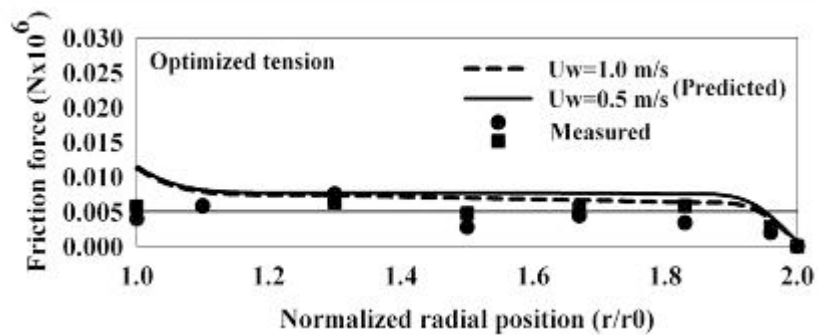
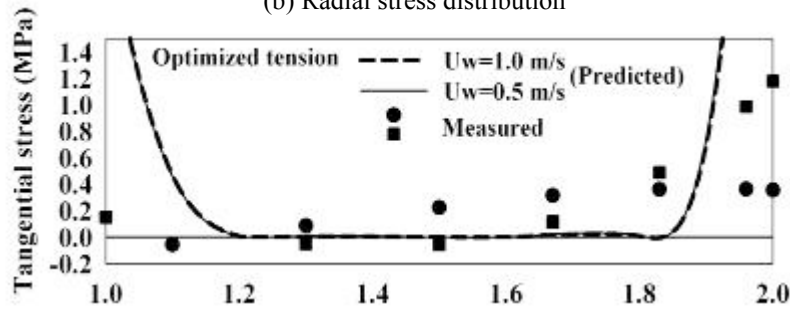


Figure 14 – Winding physical quantities under the optimized tension for nip-load=50 N,  $T_w=150$  N/m

***Optimization of Wind-up Tension of Webs  
Preventing Wrinkles and Slippage with  
Experimental Verification***

**H. Hashimoto**, Tokai  
University, JAPAN

**Name & Affiliation**

Ron Swanson, 3M  
Company

**Question**

On the charts where you discussing the starring defect the negative circumferential stress occurs out in the wound roll away from the core. But your pictures you show the buckle right outside the core. So your defect and your negative circumferential stresses do not coincide in location. What is your explanation?

**Name & Affiliation**

H, Hashimoto, Tokai  
University

**Answer**

To produce the defect seen in Figure 2a a very high winding tension was used. As a result, the radial stress near the core became large, and then such type of defect was generated.

**Name & Affiliation**

Balaji Kandadai,  
Kimberly-Clark  
Corporation

**Question**

On your tangential stress plots, you show measured values. Is that actually measured or inferred from radial pressure measurements and the stress equilibrium equation?

**Name & Affiliation**

H. Hashimoto, Tokai  
University

**Answer**

You are correct; I haven't measured the tangential stress directly. I measured only the radial stress. The force balance equation was applied to calculate these values.

**Name & Affiliation**

Michael Desch, Technical  
University of Darmstadt

**Question**

Just for clarification, what are your variables in your optimization? Were the variables only the tension on the web or the nip load? Or both?

**Name & Affiliation**

H. Hashimoto, Tokai  
University

**Answer**

In this case I only adjusted the winding tension. I've tried to adjust both tension and nip load.